Pilot-scale hydrothermal pretreatment and optimized saccharification enables bisabolene production from multiple feedstocks

Journal:	*Green Chemistry*
Manuscript ID	GC-ART-01-2019-000323.R2
Article Type:	Paper
Date Submitted by the Author:	07-May-2019
Complete List of Authors:	Perez-Pimienta, Jose; Universidad Autonoma de Nayarit, Chemical Engineering Papa, Gabriella; E O Lawrence Berkeley National Laboratory, Biological Systems and Engineering Rodriguez, Alberto; Joint BioEnergy Institute, Deconstruction; Sandia National Laboratories, Barcelos, Carolina; Joint BioEnergy Institute Liang, Ling; E O Lawrence Berkeley National Laboratory, Stavila, Vitalie; Sandia National Laboratories, Engineered Materials Department, MS-9161 Sanchez, Arturo; Centro de Investigación y Estudios Avanzados (CINVESTAV) Gladden, John; Joint BioEnergy Institute, Deconstruction Simmons, Blake; E O Lawrence Berkeley National Laboratory, Biological Systems and Engineering

Green Chemistry

PAPER

Pilot-scale hydrothermal pretreatment and optimized saccharification enables bisabolene production from multiple feedstocks

Received 00th January 20xx,
Accepted 00th January 20xx

DOI: 10.1039/x0xx00000x

José A. Pérez Pimienta[a,b,*], Gabriella Papa [c], Alberto Rodriguez[c,d], Carolina A. Barcelos[c], Ling Liang [e], Vitalie Stavila[f], Arturo Sanchez[a], John M. Gladden[c,d], and Blake A. Simmons[c]

To date, information on biomass deconstruction and advanced biofuels production using pilot-scale pretreatments is scarce and typically derived from single feedstocks, making comparisons complicated. This work evaluates the effect of subjecting four different feedstocks (agave bagasse [AG], corn stover [CS], sugarcane bagasse [SC] and wheat straw [WS]) to pretreatment at 180 °C for 20 min in a 200 kg/day pilot-scale continuous tubular reactor constituted by three sequential stages (compression, autohydrolysis and steam explosion). Correlations between the structural changes and differences in digestibility on pretreated biomass were determined. It was determined that xylan removal by pretreatment generated more crystalline and energy dense materials, with higher lignin content and S/G ratio. Optimal reaction conditions for enzymatic saccharification of pretreated feedstocks at lower enzyme doses generated glucose conversions up to 80%. Finally, it was demonstrated that the yeast *Rhodosporidium toruloides* was able to grow in all hydrolysates, exhibiting simultaneous C_5 and C_6 sugars consumption and bisabolene production.

Introduction

Lignocellulosic biomass (LCB) has the potential to serve as a key resource for the production of second-generation biofuels and chemicals, partially contributing to substitute petroleum-derived products [1]. Pretreatment is required to decrease the recalcitrance and increase the digestibility of LCB. Hemicellulose acts as a blocking seal limiting enzyme access to the cellulose–hemicellulose complex while lignin forms a physical barrier that increases resistance to chemical and microbial attack, hindering polysaccharide hydrolysis into monomeric sugars [2].

To date, various pretreatment processes have been developed, and can be broadly categorized into physical, chemical, biological, and combined approaches [3]. The vast majority of these pretreatments have only been tested at laboratory scale (1-10 g/h) and usually in batch mode (e.g. ozonolysis or biological pretreatment using fungi), resulting in an extensive characterization of their impact to structure, digestibility and fermentability properties of different types of LCB [4]. On the other hand, pilot-scale pretreatment systems (1-5 kg/h) aim to provide performance data that can more reliably be applied to process scale-up, by considering and imitating the equipment configuration and capabilities of commercial-scale pretreatment systems [5]. The use of large-scale continuous reactors is desirable when processing large quantities of LCB, which is often neglected in laboratory scale investigations. However, continuous systems have proven particularly difficult to design and operate effectively with high solids loadings (> 15% insoluble solids) [6]. Due to the technical difficulties associated with the operation of pilot-scale continuous tubular reactors (PSR), literature reports on their performance (structural characterization of pretreated solids, sugar yield and biofuel production) are scarce, usually employ only one feedstock, and provide limited information on biofuel production potential [7,8].

With this in mind, a PSR that can operate at a 200 kg dry mass per day basis was designed and constructed at CINVESTAV. After initial testing, this PSR proved capable of handling multiple feedstocks at high solids loading (i.e >20%), to potentially increase sugar/ethanol concentrations and decrease total costs [9]. The PSR comprises three individual and sequential stages (compression, autohydrolysis and steam explosion) and, importantly, liquid water is the only solvent used during pretreatment. The biomass enters the screw conveyor chamber equipped with a plug-screw feeder to compress the biomass into a densified plug, which serves as a pressure-sealing barrier inside the reactor and leads to a compression process that involves high shear for pulverization. Secondly, within the reactor chamber, the densified biomass plug reacts at a specific temperature/pressure (i.e. 180°C and ~145 psi) in an autohydrolysis

[a] Laboratorio de Futuros en Bioenergía, Unidad Guadalajara de Ingeniería Avanzada, Centro de Investigación y Estudios Avanzados (CINVESTAV), Zapopan, Mexico.
[b] Department of Chemical Engineering, Universidad Autónoma de Nayarit, Tepic, Mexico. Email: japerez@uan.edu.mx
[c] Joint BioEnergy Institute, Biological Systems and Engineering Division, Lawrence Berkeley National Laboratory, Emeryville, CA, United States.
[d] Department of Biomass Science and Conversion Technology, Sandia National Laboratories, Livermore, CA, United States Address here.
[e] Advanced Biofuels Process Demonstration Unit, Lawrence Berkeley National Laboratory, Berkeley, CA, United States
[f] Energy Nanomaterials Department, Sandia National Laboratories, Livermore, CA, United Stated
† Electronic Supplementary Information (ESI) available.

process that typically results in the removal of xylan and rearrangement of lignin [10].

Finally, at the reactor outlet, the biomass is steam exploded into a blow tank where the pretreated biomass is recovered. This rapid pressure release is known to cause additional biomass defibrillation [11]. As a result, this system features rapid contact with the catalyst and promotes effective heat and mass transfer, enabling it to be used in continuous operation mode.

While ethanol production from pilot-scale pretreated biomass has been previously demonstrated [8,12,13], limited information exists on the production of advanced biofuels including molecules suitable as D2 diesel and jet fuel precursors. One example is the development of an ionic liquid-based process for production of the sesquiterpene bisabolene at benchtop and pilot bioreactor scales by an engineered strain of *Rhodosporidium toruloides*, which is an oleaginous yeast that can readily consume glucose, xylose and aromatic lignin decomposition products [14]. While high product titers were achieved in that work, it is desirable to explore and compare other types of biomass feedstocks and cost effective alternative pretreatments that can be promising in terms of reduced downstream toxicity.

In the present study, we explored bisabolene production by cultivating the same strain of *R. toruloides* in hydrolysates derived from PSR pretreated biomass using four different feedstocks: agave bagasse (AG), corn stover (CS), sugarcane bagasse (SC) and wheat straw (WS), at a constant temperature (180 °C) and residence time (20 min). In order to decrease enzyme usage during saccharification of all four pretreated feedstocks, a central composite design (CCD) of response surface methodology (RSM) was designed to identify optimal saccharification conditions (temperature, pH, and enzyme loading). The best conditions were then applied to generate hydrolysates that were tested for their biocompatibility as cultivation media for the production of bisabolene. Also, a systematic structural characterization on the pretreated biomass sources and its relevance for digestibility was carried out using correlation methods. Cellulose crystallinity was determined by X-ray diffraction (XRD), the energy density (ED) was determined by calorimetry, and the molecular weight distribution was obtained by gel permeation chromatography (GPC). Finally, the ratios of syringyl (S) to guaiacyl (G) aromatic compounds constituting the lignin were determined by pyrolysis gas chromatography mass spectrometry (Py-GC/MS).

Experimental

Biomass samples and preparation

The biomass feedstocks were obtained from diverse agro-industrial sources in Western Mexico. All LCB were milled using an Azteca knife and hammer mill (Proinco, Mexico) with a 0.5 in screen size. Compositional analyses of the pretreated solids were performed using the standard analytical procedures of the National Renewable Energy Laboratory (NREL) by the two-step sulfuric acid hydrolysis method (NREL/TP-510-42618) [15].

Continuous pilot-scale pretreatment

Biomass pretreatment was carried out in a 200 kg/day PSR constituted by three stages (compression, autohydrolysis and steam explosion) (Figure 1). Soaked biomass at a 1:10 biomass/water ratio (w/w) was fed into the reactor via a plug screw feeder, then squashed, compacted by the screw, and gradually heated in a conveyor screw at 180 °C using saturated steam with a 20 min residence time. Finally, the biomass was pushed through the reactor to reach two steam explosion valves and a blow tank, where the hydrolysate is separated into a high solids pretreated slurry (~30% w/w) while exhausting steam. After pretreatment, the samples were cooled down to room temperature, weighted and their moisture content was determined. Only the solid fraction was investigated. The pretreated solids were washed with 30 g of deionized water per g of biomass, milled using a 20 mesh screen size, and stored at 4 °C for further analysis.

Optimization of enzymatic saccharification

Experimental design

To determine the optimal process conditions for each of the four pilot-scale pretreated agroindustrial residues, a central composite design (CCD) using response surface methodology (RSM) was used. Temperature, pH and enzyme loading were chosen as independent variables and glucose conversion used as response.

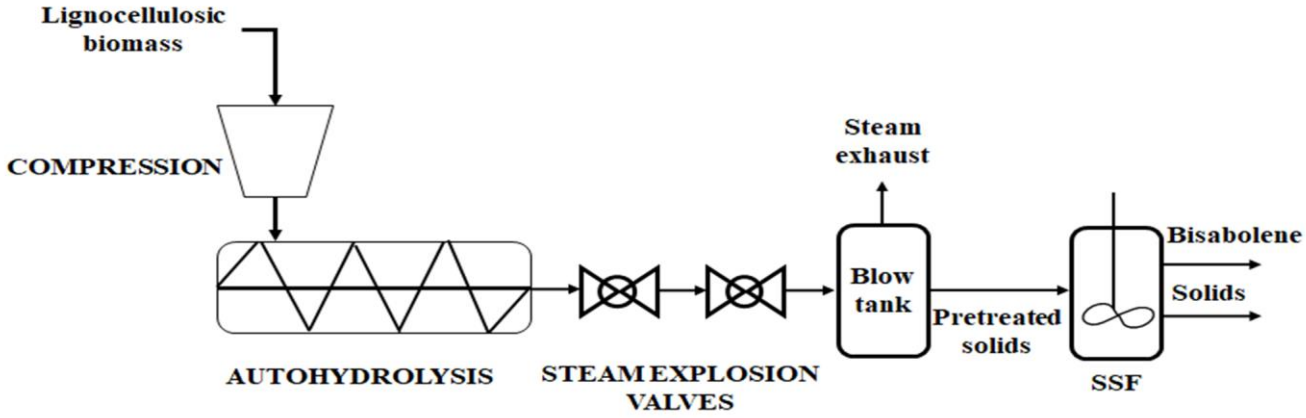

Figure 1. Process flow diagram of the pilot-scale continuous tubular reactors (PSR) for the pretreatment of four feedstocks (agave bagasse, corn stover, sugarcane bagasse and wheat straw) for the production of bisabolene.

The experimental data were fit using the following polynomial quadratic equation:

$$y = \beta_0 + \sum_{i=1}^{3} \beta_i X_i + \sum_{i=1}^{3} \beta_{ii} X_i^2 + \sum_{i=1}^{3} \sum_{j=i+1}^{3} \beta_{ij} X_i X_j \qquad (1)$$

where y is the response, X_i and X_j are independent variables, β_0 is the constant coefficient, β_i is the ith linear coefficient, β_{ii} is the quadratic coefficient, and β_{ij} is the ijth interaction coefficient. CCD consists of 2k factorial points, 2k axial points (±α), and six central points, where k is the number of independent variables. The experimental design comprised 20 runs with six replicate runs at the center point and six axial points per pretreated biomass (Table 1). The results were analyzed using Design Expert 10.0.1 including ANOVA to obtain the impact and significance of each term and the interactions between the process variables and response. The fit quality of the polynomial model was expressed via the determination coefficient, R^2, and its statistical significance was verified with the F-test using the same software program.

Table 1. Levels of the enzymatic saccharification variables evaluated in the CCD.

Variable	Unit	Coded levels				
		-α[a]	-1	0	1	-α[a]
Temperature	°C	45.0	48.1	52.5	57.0	60.0
pH		4.50	4.81	5.25	5.70	6.00
Enzyme loading	mg enzyme protein/g glucan	5.0	14.1	27.5	40.9	50.0

[a]α (axial distance) = $\sqrt[4]{N}$, where N is the number of experiments of the factorial design. In this case, 1.6818.

Enzymatic hydrolysis

Enzymatic saccharification of pretreated samples were carried out in a rotary incubator (Enviro-Genie, Scientific Industries, Inc.) using 50 mM citrate buffer for 24 h at 1% solids loading using the specific process conditions accordingly to the experimental design run (T, pH and enzyme loading). An enzyme mixture of Ctec3 and HTec3 (Novozymes, Franklinton, NC, USA) at ratio of 9:1 v/v was used. Protein content of enzymatic cocktails were 107.7 ± 2.1 mg/mL and 80.4 ± 5.4 mg/mL protein for CTec3 and HTec3, respectively. Reactions were monitored by removing 100 µL of the supernatant and measuring the glucose and xylose concentration with an YSI analyzer, as described below. The cellulose to glucose conversion used in the CCD (referred simply as glucose conversion) was calculated as previously described [16].

Bisabolene fermentation

Batch reactions at high solids loading

Enzymatic saccharification reactions for each pretreated biomass were carried out at their specific optimum process conditions (combination of temperature, pH and enzyme loading), using 20% solids loading during 72 h to obtain a stream with high concentration of sugars for bisabolene fermentation.

Upon completion of the saccharification reaction, the unhydrolyzed biomass was separated from the liquid fraction by two sequential centrifugation steps at 10000×g for 10 min. The liquid fraction was supplemented with synthetic defined (SD) medium, which was prepared as a 10x stock by mixing yeast nitrogen base without amino acids (BD Difco, USA) and complete supplemental mixture (Sunrise science products, USA) according to manufacturers' instructions. The pH of the supplemented hydrolysates was then adjusted to 7.5 by addition of 5 M NaOH, filtered through 0.45 µm membranes and stored at 4 °C until use. *Rhodosporidium toruloides* BIS3 strain was used for all fermentations in this study (JBEI registry ID: JBx_065244). This bisabolene-producing strain was engineered from wild-type *R. toruloides* strain IFO0880, obtained from the NBRC culture collection, as previously reported [17]. Seed cultures were prepared by transferring strain BIS3 from a YPD agar plate into tubes containing 10 mL of YPD media, and grown overnight at 30 °C and 200 rpm shaking speed. Cells were then diluted ten times with fresh YPD medium, grown under the same conditions until mid-exponential phase, and inoculated at an initial OD_{600} of 0.2 into glass cultivation tubes containing 10 mL of the hydrolysates and a 2-mL dodecane overlay. Growth was monitored by measuring OD_{600} using a SpectraMax M2 spectrophotometer (Molecular Devices, USA) and disposable cuvettes, after brief centrifugation and resuspension of cells with sterile water. Samples from the supernatant and the dodecane overlay were collected and stored at -20 ºC for sugars and bisabolene analysis, respectively. All assays were performed in triplicate and the data are reported as the mean ± standard deviation.

Pulse-feeding saccharification experiments at high solids loading

With the goal of obtaining higher product titers by increasing the initial monomeric sugar concentrations, pulse-feeding saccharification reactions by using pretreated WS under optimal process conditions were performed.

The pulse-feeding strategy during enzymatic saccharification was implemented to an initial reaction with 20% solids loading for 24 h, by the sequential addition of 5% solids equivalent at specific time intervals, up to 35% solids loading. The enzyme dosage ratio was maintained at 28.8 mg/g glucan throughout the process (120 h total). After reaction completion, the hydrolysate was prepared for fermentation and bisabolene production, as in the batch reactions experiments. All assays were performed in triplicate and the data are reported as the mean ± standard deviation.

Analysis

Quantification of sugars and bisabolene

Glucose and xylose concentrations in the supernatants were determined with a YSI 2900 Biochemistry Analyzer (Xylem, USA), equipped with glucose oxidase (YSI 2365) and xylose oxidase (YSI 2761) membranes, and buffer solution (YSI 2357). Automatic calibrations were performed using glucose/lactate (YSI 2776, 2.5 g/L glucose) and xylose (YSI 2767, 20.0 g/L) calibration solutions, and the linearity was tested with external standards. All samples were

centrifuged and filtered through 0.45 µm filters, and diluted with water before analyses.

To quantify bisabolene, samples from the dodecane overlay were diluted into ethyl acetate spiked with 5 mg/L caryophyllene and analyzed by gas chromatography-mass spectrometry (GC-MS), using an Agilent Technologies 6890N system, equipped with a 5973 mass selective detector and a DB-5ms column (30 m x 250 µm x 0.25 µm, Agilent Technologies, USA). Splitless 1 µL injections were used on a GC oven program consisting on 100 ºC for 0.75 min, followed by a ramp of 40 °C per min until 300 ºC, and held 1 min at 300 °C. The injector and MS quadrupole detector temperatures were 250 °C and 150 °C, respectively. Bisabolene concentrations were calculated by integration of the peak area values obtained in selective ion monitoring mode, compared to a calibration curve made with pure bisabolene, and normalized with the areas obtained from the spiked caryophyllene, as internal standard. Bisabolene concentrations in the dodecane layer were adjusted to represent the concentrations in the aqueous volume of the cultures.

Gel-permeation chromatography (GPC)

The molecular weight distributions of the biomass feedstocks were determined by GPC from the untreated and pretreated samples. These measurements were carried out using a Tosoh Ecosec HLC-8320 GPC equipped with a UV detector, whose wavelength was set at 280 nm. The mobile phase consisted of tetrahydrofuran (THF) with 250 ppm of butylated hydroxytoluene (BHT), and the column used was an Agilent PLgel 3 µm 100 Å (300 × 7.5 mm). The column flow rate was 1.0 mL/min at 35 °C, and the injection volume was 50 µL. Polystyrene standards were purchased from Agilent (Agilent Technologies, Inc., Santa Clara, CA) and used to establish a calibration curve that ranged from 162 to 29, 150 g/mol. Prior to analysis, all samples were derivatized with a mixture of acetic anhydride and pyridine (1:1 v/v) for 24 h at 37 °C. This mixture was evaporated under a flow of nitrogen gas, and the samples were resuspended with 1.5 mL of THF and filtered using 0.2 µm polytetrafluoroethylene (PTFE) filters, prior to injection.

Three separate samples were prepared and analyzed for each biomass type and condition. The molecular weight distribution graphs display the average values obtained.

Crystallinity measurement

XRD diffractograms of untreated and pilot-scale pretreated biomass were acquired with a PANalytical Empyrean diffractometer equipped with a PIXcel3D detector with Cu Kα radiation. The samples were scanned in the range of 5–50° (2θ) with a step size of 0.026° at 45 kV and 40 mA under ambient temperature. Crystallinity index (CrI) was calculated by using the following equation:

$$CrI = \frac{I_{002} - I_{am}}{I_{002}} \quad (2)$$

where I_{002} is the intensity for the crystalline portion of biomass at about 2θ = 22.4, and I_{am} is the peak for the amorphous portion.

Energy density

The energy content of untreated and pretreated biomass in the PSR (20 min and 180 °C) was measured using an oxygen bomb calorimeter (IKA C2000, Wilmington, NC, USA). The bomb calorimeter was calibrated using a known amount of standard benzoic acid (Sigma-Aldrich, St. Louis, MO, USA). Intrinsic to the method, ΔT_{std} represents the recorded rise in temperature of benzoic acid during combustion. The term ΔT_{sample} represents the recorded rise in temperature after combustion of the pelleted biomass samples. The ED of the samples was calculated based on the following equation:

$$ED = ED_{BA} * \frac{W_{AB} * \Delta T_{sample}}{W_{sample} * \Delta T_{std}} \quad (3)$$

where, ED is energy density of sample, ED_{BA} is the energy density of benzoic acid, W_{BA} is the weight of benzoic acid, and W_{sample} is the weight of sample. Ash weight was measured by subtracting the weight of the crucible before and after bomb calorimetry. ED calculations were adjusted by subtracting the moisture and ash content, using the following equation:

$$ED_a = \frac{ED_{sample}}{(1 - ash\%)} \quad (4)$$

where, ED_a is the energy density of the sample "ash-free". This adjustment ensured that energy was accounted only to the cellulose, hemicellulose, and lignin fractions of the samples.

Pyrolysis-GC/MS

The ratio between syringyl and guaiacyl lignin monomers was determined in untreated and pretreated samples by pyrolysis coupled with gas chromatography mass spectrometry.

Samples of 0.5 mg were pyrolyzed at 550 ^{o}C using the pyroprobe 5200 (CDS Analytical, Inc., Oxford, PA, USA) connected to a gas chromatography mass spectrometry (GC/MS) system (Agilent 6890) composed of a Trace GC Ultra and a Polaris-Q MS (Thermo Electron Corporation, Waltham, MA, USA) equipped with a TR-SMS column (60 m 0.25 mm ID 0.25 lm) and operated in split mode (40 mL min^{-1}) using He as carrier. The chromatograph program was set as follows: 5 min at 50 °C, followed by an increase of 5 °C min^{-1} to 300 °C, finally maintained at 300 ^{o}C for 5 min. Pyrolysis products were identified on the basis of their mass spectra using the NIST08 mass spectrum library. Compounds of syringyl (S), guaiacyl (G) and *p*-hydroxyphenyl (H) origin were quantified from the pyrogram using the peak area. The S/G ratio was calculated as the sum of all peak areas of S molecules divided by the sum of all peak areas of G molecules. The relative area percent for each chromatographic peak was employed as a semi-quantitative approach to evaluate the contribution of each S and G compound area to the total peak area. The lignin S/G ratios were determined using the relative areas of the fragments from the pyrolysis of lignin guaiacyl and syringyl types (21 compounds, Table S1).

Table 2. Chemical and physical characteristics of the 4 biomasses studied: composition (% dry matter), crystalline indexes (CrI), Energy density (ED), lignin syringyl/ guaiacyl ratio (S/G) ratio, and molecular weight (MW) determined untreated and CPR-pretreated biomass.

Biomass	Process	% Glucan	% Xylan	% Lignin	CrI (%)[1]	ED (MJ/kg)[2]	Lignin subunits		S/G ratio[4]	MW (g/mol)[5]	Pd[6]
							% S[3]	% G[3]			
Agave bagasse	Untreated	31.6±0.3	24.0±0.3	18.6±0.1	24.7	16.4	51.8	48.2	1.07	1070	3.7
	Pretreated	42.9±0.3	12.6±0.2	26.6±0.3	26.3	17.9	62.1	37.9	1.64	29824	48.4
Corn stover	Untreated	33.1±0.1	25.7±0.8	18.3±0.4	34.8	15.8	27.8	52.4	0.53	2003	3.2
	Pretreated	46.5±0.2	20.5±0.3	24.7±0.2	39.5	17.4	27.4	51.9	0.53	27995	29.5
Sugarcane Bagasse	Untreated	42.1±0.3	25.7±0.5	22.7±0.1	36.8	17.2	31.0	49.1	0.63	2485	3.8
	Pretreated	54.2±0.1	12.6±1.8	25.9±0.0	41.2	17.4	36.6	40.6	0.90	25665	31.0
Wheat straw	Untreated	32.6±0.1	25.6±1.0	19.1±1.2	40.1	15.2	30.6	63.1	0.49	1340	3.2
	Pretreated	47.9±0.1	17.3±0.5	24.3±0.2	44.3	16.2	38.7	56.4	0.69	29606	34.6

[1] CrI = Crystallinity index of cellulose determines by X-ray diffraction (XRD)
[2] ED = Energy density determined by bomb calorimeter
[3] Lignin subunits= syringyl (S) and guaiacyl (G)
[4] Syringyl (S) and guaiacyl (G) lignin subunits ratio determined by Py-GC/MS
[5] MW = Average molecular weight determined by gel permeation chromatography (GPC)
[6] Pd = Polydispersity determined by gel permeation chromatography (GPC)

Statistical analysis

The bisabolene production was analyzed for statistical significance by a one-way ANOVA and Tukey test (P<0.05). Finally, the structural characteristics, cell wall components and its relation with biomass digestibility was evaluated using regression modeling (R^2) and the Pearson's correlation coefficient (r) with a statistical significance of P<0.05 and 0.01.

Results and discussion

Compositional analysis of pretreated biomass samples

To be able to better assess the effects of pretreatment, the main components of lignocellulosic biomass (glucan, xylan and lignin) were monitored and quantified. The compositions observed for the untreated samples were consistent with previous reports and displayed low variability among the different sources, in the range of 31.6-42.1% for glucan, 24.0-25.7% for xylan and 18.3-22.7% for lignin [16,18]. After PSR pretreatment, a fraction of xylan was removed from the plant cell wall and a relative increase in lignin content was observed as a consequence (Table 2). Interestingly, up to 51% of xylan was removed in SC, but only ~20% in CS, which shows that the biomass source is still a determinant factor under the conditions evaluated here. Even though lignin is reported to be affected by steam explosion pretreatment, the lignin effect was minor with respect to hemicelluloses removal, in agreement with previous findings [19]. Only limited information on component removal after pretreatment at a pilot-scale in similar conditions is available in the literature with most reports employing dilute acids (0.7-2.4% H_2SO_4) and temperatures below 190 °C. Recently, McIntosh et al. [(2016)] used a 200 kg/day PSR with Eucalyptus (180 °C, 15 min, 2.4% H_2SO_4) and achieved a xylan reduction of 73.6%. Similarly, Wang et al. [(2014)] investigated the pretreatment of corn stover in a 200 kg/day PSR (160 °C, 20 min, 2.0% H_2SO_4) and showed 85.4% of xylan removal. These differences could be attributed to the acid conditions during pretreatment, however, if not carefully controlled, they can also result in degradation of sugars and generation of fermentation inhibitors [20]. The difference in xylan removal yields between dilute acid and hydrothermal pretreatments is well documented [10], however, the evaluation of reactor configurations at the pilot-scale is important to determine the changes in process performance as a result of scale-up and the use of different feedstocks. These results contribute to the understanding of pilot-scale pretreatment systems that are based on hydrothermal process without additional chemicals (acids or alkali).

Cellulose crystallinity measurements

X-ray diffraction was used to determine the cellulose crystallinity (CrI), which has been reported to affect enzymatic saccharification efficiency [21]. A comparison between the diffraction patterns of the untreated and PSR-pretreated biomass is shown in ESI Figure S1. The patterns from CS, SC and WS display the typical lignocellulosic pattern with a sharp cellulose peak at 22.5° and a lower and broader peak at ~15.9°. Only AG displays prominent calcium oxalate peaks at 2θ = 15°, 24° and 30.5°, as previously reported [22]. After pretreatment, all samples presented a more intense cellulose peak, which corresponds to increased crystallinity and higher CrI (Table 2). The largest CrI increase was obtained in CS from 34.8% to 39.5%, while in AG it was only from 24.7% to 26.3%. It has been reported that after an autohydrolysis pretreatment (where water acts as an acid at high temperature and pressure), cellulose hydrolysis and removal from the amorphous regions and subsequent solubilization of glucose can increase CrI values [23].

Other reports have shown that a more efficient enzymatic saccharification with an increased CrI may be due to the relatively low hemicelluloses proportion or smaller non-crystalline cellulose region, where it is proposed that lignin interact with hemicelluloses rather than with cellulose (preferential removal of hemicelluloses *vs* cellulose) which may directly reduce hemicelluloses cross-linking to cellulose [19,24]. Furthermore, it has been found than in autohydrolysis-based pretreatments at 180 °C, there is a rupture of the glycosidic bonds within the crystalline cellulose while for amorphous cellulose this occurred at 150 °C [25]. The increase in CrI in the pretreated biomass indicates that recovered products are more crystalline and along with other structural features would enable a specific enzymatic digestibility for each biomass type.

Lignin S/G ratios and aromatic compounds in untreated and pretreated biomass

One of the major structural features that impact biomass recalcitrance is the lignin S/G ratio, which can influence the cross linking between lignin and other cell wall constituents, modifying their microscopic structure, topochemistry, and the accessibility of the cell wall to enzymes [19]. This parameter may help to predict cell wall degradability, as some studies have reported that a higher amount of S-type lignin can increase sugar yields during enzymatic saccharification [26]. For example, pine has a 0.01 S/G ratio and is considered one of the raw materials of greatest difficulty for conversion into sugars [27]. However, other reports have not found a good correlation of S/G ratio with biomass digestibility, suggesting that the S/G ratio may contribute differently to biomass recalcitrance, depending on the feedstock type and pretreatment conditions [28].

The S/G ratios observed for the untreated biomasses studied in this work were 1.07, 0.53, 0.63 and 0.49 for AG, CS, SC and WS, respectively (Table 2). These results are in concordance with previously reported values [AG (1.57), CS (0.5), SC (1.1), and WS (0.5)] [29–31]. The PSR pretreatment increased the S/G ratio in all samples, where AG showed the highest increase from 1.07 to 1.64, with the exception of CS that remained at the same level. As suggested by previous studies with other pretreatments (i.e. alkali and kraft pulping), the S-lignin is easy to deconstruct, in contrast with acid-based processes where G-lignin is easier [32]. In general, more S-lignin is better for acid digestibility but not for enzymatic hydrolysis of sugars, and this may be the reason why an increase in S/G was observed for most of the samples. As PSR pretreatment resembles an acid-based pretreatment, it needs to take into consideration the contributions of the grinding action of the reactor mixing screws and rapid decompression effects during steam explosion. The semi-quantitative approach employed was able to evidenced general trends in S/G ratio after pretreatment and interestingly, these values are the first ever report of S/G ratio from PSR-pretreated solids

A possible route for the formation of guaiacol and syringol is the cleavage of the aryl-alkyl-aryl ether linkage (β-O-4 bond) in lignin during pyrolysis. Syringol and guaiacol are derived from the saturated side chain structure such as 4-methylguaiacol and 4-methylsyringol, possibly formed by the cleavage of the C-C bond in the side chain.

The high content of syringol and its derivatives is primarily due to the fact that the β-O-4 bond between syringil units is easier to cleave than for guaiacyl units [33]. The pyrolytic products of lignin are shown in ESI Table S1. The percentile relative abundance of the main aromatic compounds detected by Py-GC/MS in untreated and PSR-pretreated biomass are shown in ESI Figure S2. Significant differences in aromatic compound composition were observed between untreated and pretreated samples for each type of biomass. The compound with the highest relative abundance in all materials was the 4-allyl-2,6-dimethoxyphenol (S-lignin), representing 16.0-36.0% of the detected compounds. There are no reports available regarding the pyrolytic products of *Agave tequilana* bagasse, however, two previous reports with *Agave sisalana* are in agreement with some compounds such as acetosyringone and syringol among others [33,34].

A reduction or complete removal of specific recalcitrant compounds (i.e. 3-tert-butyl-4-hydroxyarisole) after pretreatment could result in a lower recalcitrance and increased enzymatic digestibility. The most relevant G-lignin aromatic compounds formed after pretreatment in all feedstocks were vanillic acid and isovanillin while others obtained a relative increase (i.e. isoeugenol and 3-allyl-6-methoxyphenol). Finally, the untreated SC had the highest relative abundance from the evaluated LCB with some compounds of interest from G-type monomers such as vanillic acid, 2,6-dimethoxy-4-(2-propenyl) and 2,6-dimethoxyphenol. The chemical conversion of different types of lignin-derived compounds that may act as enzyme inhibitors by pretreatment is a promising area to improve the productivity and yields of deconstruction processes. However, more in-depth studies must be performed to determine if changes in the concentrations of released phenolics have a positive or negative impact on saccharification and fermentation [35].

Effects on energy density

The energy potential from biomass is useful for calculations on predicted bioenergy output by direct combustion of thermal systems and fermentation calculations. The ED and EDa from untreated and pretreated biomass are shown in Table 2. Pretreatment in the PSR increased the energy density of all LCB. This change can be attributed to the steam explosion making structural changes to the LCB and breaking down lignin into lower molecular weight products (as seen with Py-GC/MS). The highest energy density of the untreated biomass was obtained with SC (17.2 MJ/kg), while the lowest was obtained with WS (15.2 MJ/kg). These values are among those previously reported for the evaluated LCB such as AG with 16.4 MJ/kg, CS with 17.96 MJ/kg, SC with 17.8 MJ/kg, and WS with 17.3 MJ/kg [22,36–38]. The most significant increase after pretreatment occurred in CS from 15.8 to 17.4 MJ/kg, in contrast to SC that only increases from 17.2 to 17.4 MJ/kg. However, when the energy density is taken in an ash-free base (EDa) to quantify only the organic fraction present, relevant changes are noticed mainly in the WS and CS indicating greater uniformity of values for the untreated biomass from 16.9 to 17.7 MJ/kg and pretreated biomass with 17.7 to 18.6 MJ/kg, whereas AG obtained the highest EDa with 18.6 MJ/kg. Elemental composition and its variation in cell wall composition and ash is strongly correlated with ED and EDa [36].

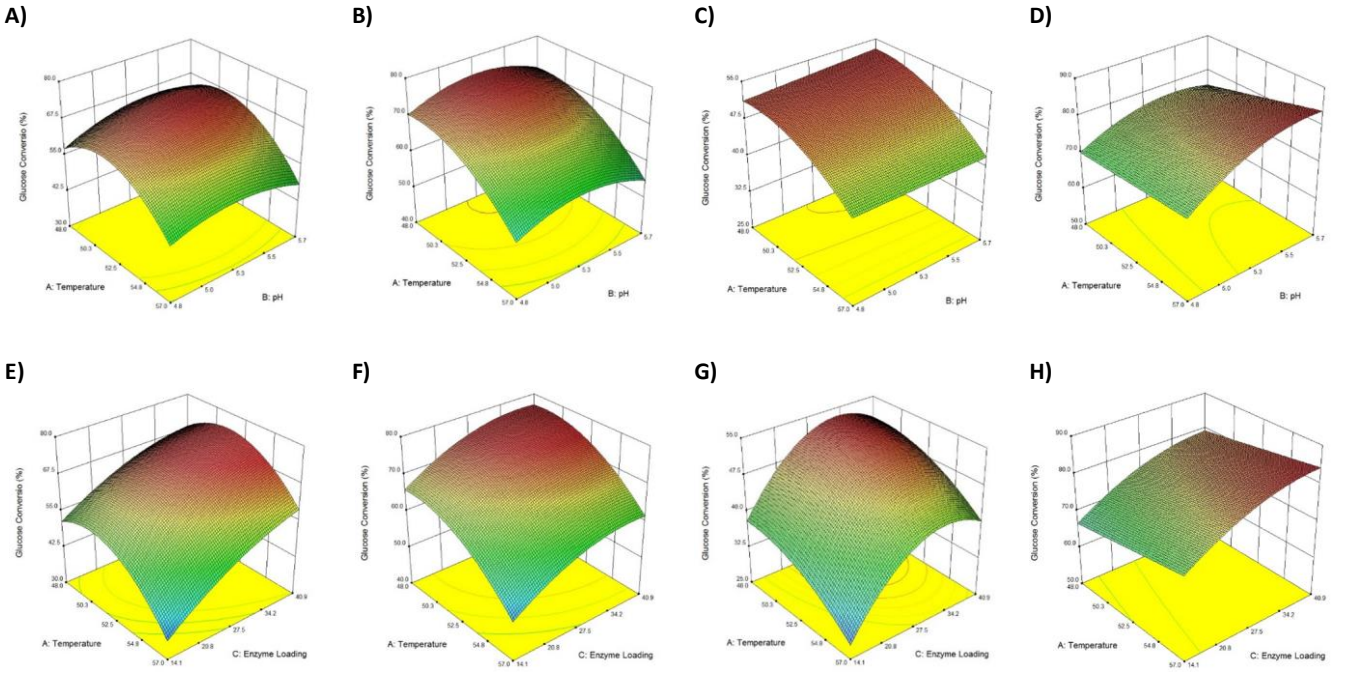

Figure 2. Response surface plots showing the effects of glucose conversion (%) and temperature (°C) on pH (A-D) and enzyme loading (mg/g glucan) (E-H) from PSR-pretreated agave bagasse (A and E), corn stover (B and F), sugarcane bagasse (C and G), and wheat straw (D and H).

Lignin proportion in biomass can be used as an ED indicator due to its relatively lower oxygen concentration than glucan and xylan [39]. Possibly due to its initial higher lignin content, the ED for SC did not significantly increase after pretreatment, in contrast to AG and CS.

Comparison of the molecular weight distributions in untreated and pretreated biomass

Changes to lignin molecular weight distribution were monitored by gel permeation chromatography (GPC) for untreated and pretreated biomass, as shown in Table 2 and ESI Figure S3. All untreated samples showed much lower UV intensity (280 nm) than the corresponding pretreated samples. Considering that a similar amount of biomass was used throughout, the drastic increase in the calculated MW values after pretreatment may seem counterintuitive at first. However, this effect is likely a consequence of the increase in the solubility of lignin in the employed solvent (THF) by the pretreatment, indicating structural changes in the LCB. As a result, the average molecular weights of the untreated biomass were in the range of 1070 to 2485 g/mol while the pretreated samples increased considerably, ranging from 25665 to 29824 g/mol (Table 2). At least three discrete zones in the MW distribution profiles can be compared: a defined peak around 200 Da, and two broader peak regions around 1500 and 5000 Da. The peak at 200 Da, which likely corresponds to lignin-derived monomers, increases after pretreatment in CS or WS, but not in AG or SC, where it is already present in the untreated samples (ESI Figure S3). Compared to AG, pretreatment in the other LCB resulted in higher peaks at 1500 and 5000, and similar Mw distributions between CS, SC and WS. On the other hand, the polydispersity index (Pd) provides an estimate of the molecular weight distribution in a polymeric material.

The Pd did not vary significantly between untreated samples (3.2-3.8) but larger differences were found between the pretreated samples (29.5-48.4) (Table 2). Other hydrothermal pretreatments have also shown an increase in Pd and average molecular weight after the process [40]. Overall, the results show that the PSR process is changing the Mw distribution of lignin and leads to solubilization of lignin components with higher molecular weights under the tested conditions. More detailed studies should be performed to determine if the observed signal increase in the low molecular weight regions is accompanied by a corresponding degree of lignin depolymerization.

Optimization of enzymatic saccharification of PSR-pretreated biomass

Enzymatic saccharification is a key step in the conversion of biomass into ethanol or other products. In enzymatic cocktails (i.e. CTec3 and HTec3), multiple enzymes function together in a synergistic manner to perform a complete hydrolysis. However, the efficiency of digestion depends largely on the structural characteristics of the substrate (crystallinity, hemicellulose/lignin content, S/G ratio, among others) as well as temperature, pH, enzyme loading and applied process conditions. These factors often interact with each other; hence, the optimization of the enzymatic hydrolysis process plays an important role in improving the process performance. The traditional optimization method used for enzymatic hydrolysis is modifying one factor at a time while setting the other values, which makes this process laborious and often

leads to an incomplete understanding of system behaviour, factors (S/G ratio, CrI and xylan/lignin content). Nearly 80% glucose

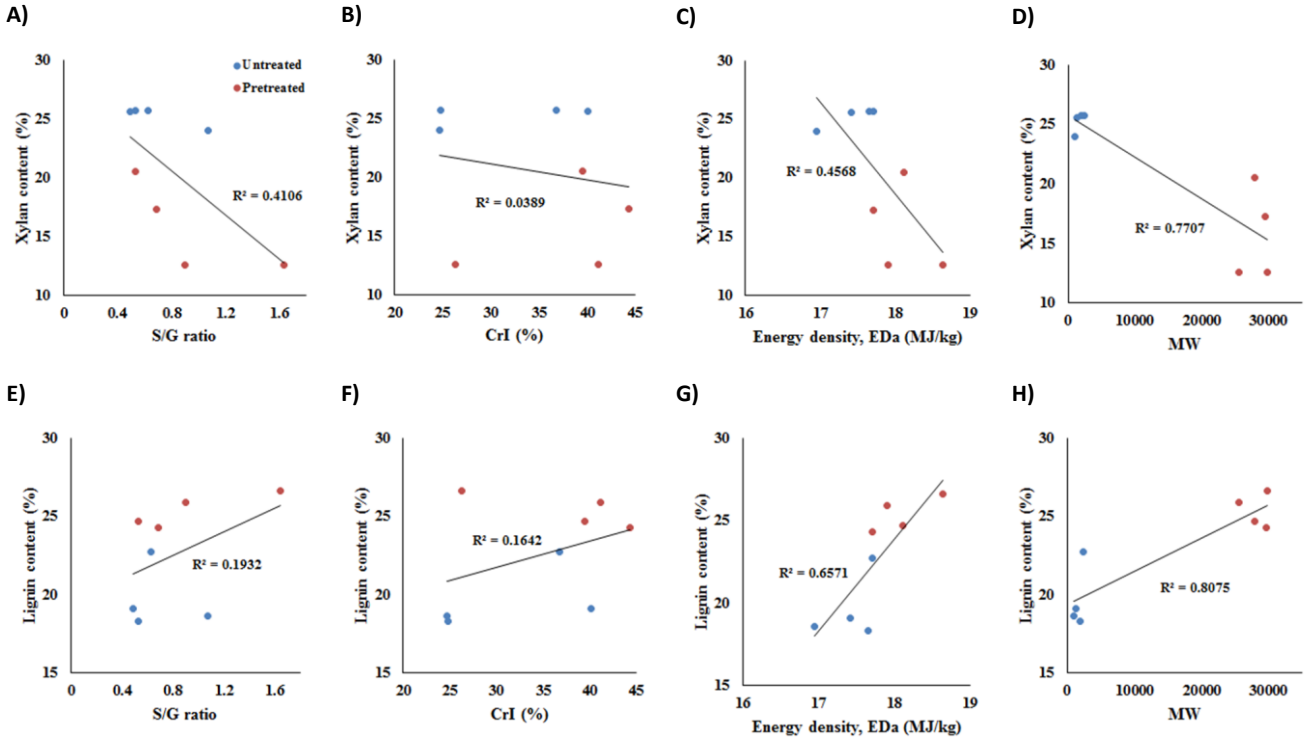

Figure 3. Correlation between S/G ratio, crystallinity index (CrI), "ash-free" energy density (EDa) and molecular weight on % xylan content (A-D), and % lignin content (E-H) from untreated and pretreated biomass. Untreated = blue points; Pretreated = red points.

resulting in a lack of predictive capacity [41].

Therefore, we chose to apply an alternative and more efficient approach with the use of a statistical method, the response surface methodology (RSM), which is a derived empirical modelling technique for the evaluation of the relationship of a set of controlled experimental factors and observed results. To optimize the enzymatic saccharification of PSR-pretreated biomass, three factors were modified, namely temperature (45-60 °C), pH (4.5-6.0) and CTec3/HTec3 enzymatic loading (5-50 mg/g glucan).

The complete design matrix and experimental results of the CCD for the four evaluated biomasses are shown in ESI Table S2, and the response surface plots are shown in Figure 2. The experimental data was analyzed to obtain a set of second-order polynomial equations that describe the conversion of cellulose to glucose. As expected, the LCB responded differently when compared to each other in terms of glucose conversion, which may be due to different conversion yield was achieved with WS while SC remained at ~ 50%. Likewise, the optimization of enzymatic saccharification conditions was focused on maximizing glucose conversion using a lower amount of enzyme than in previous reports (40 mg/g glucan) [16]. The optimized parameters of the CCD and the validation of the RSM for the PSR-pretreated biomass are shown in Table 3. The coefficients of determination (R^2) were 0.9835, 0.9755, 0.9766, and 0.9506 for pretreated AG, CS, SC, and WS, respectively. The adjusted R^2 confirms the adequacy of the model and no lack of fit was detected based on the P values. The process conditions predicted by the enzymatic saccharification models for the 4 pretreated LCB have a considerable decrease in enzyme loading (less than 30 mg/g glucan) and moderate temperatures (48.5-51.1 °C) with the exception of the WS (57.0 °C).

The predicted and validated glucose conversion values from the different samples were very similar, confirming the precision of the

Table 3. Optimized parameters and validation of the response surface model of glucose conversion from PSR pretreated biomass.

Biomass	Model parameters			Optimized parameters			Predicted glucose conversion (%)	Experimental glucose conversion (%)
	R^2	Adjusted R^2	Predicted R^2	T (°C)	pH	Enzyme loading (mg/g glucan)		
Agave bagasse	0.9835	0.9689	0.9549	51.1	5.35	29.3	69.6	72.4±2.3
Corn stover	0.9755	0.9633	0.9605	48.9	5.23	26.3	75.0	73.8±2.8
Sugarcane bagasse	0.9766	0.9682	0.9519	48.5	5.12	26.6	51.2	49.8±0.9
Wheat straw	0.9506	0.9209	0.8943	57.0	5.64	28.8	81.9	82.5±1.1

model (Table 3). The coefficient of variation between predicted and experimental values was 1-4%. Taking into consideration the optimized glucose conversion values of the LCB, they can be classified from lower to higher as: SC < AG < CS < WS. The interactions of glucose conversion with pH, temperature and enzyme loading were mainly different in their magnitude for all feedstocks. The response surface plots of AG and CS were similar when compared to SC and WS. For AG and CS, the glucose conversion was higher at a pH close to the central point, unlike SC where the pH was not decisive and similar glucose conversion was obtained for the studied range. Only in WS, the optimized glucose conversion was achieved at higher pH and temperature. Previous reports for the optimization of enzymatic saccharification based on a RSM have shown a similar or lower R^2 [42,43]. Similarly, Marcos et al. [(2012)] carried out the optimization of steam exploded WS (200 °C and 7 min), obtaining an R^2 of 0.9885 and optimized process conditions for the enzymatic cocktail Acellerase 1500 (50 ° C, pH 4 and 0.5 mL enzyme/g glucan). The PSR technology was capable to effectively pretreat different agroindustrial residues, however, in order to achieve higher sugar conversion for specific feedstocks (for example, sugarcane bagasse) more severe pretreatment conditions must be evaluated.

Correlation between biomass recalcitrance and digestibility

The different properties (S/G ratio, CrI (%), EDa and MW) from untreated and pretreated biomass were correlated to their xylan and lignin contents as well as with the glucose conversion using regression modelling and the Pearson's correlation coefficient (r) as shown in Figures 3 and 4 and ESI Tables S3 and S4.

Accordingly to a pretreatment that removes xylan, the results revealed a negative trend with the xylan content whereas a positive relationship was obtained with lignin content [45,46]. In particular, strong correlations with the MW measurements (r = -0.878; *P*<0.01; *n* = 8; r = 0.899; *P*<0.01; *n* =8, for xylan and lignin respectively) were found due to newly condensed structures of lignin in the pretreated biomass [47]. Significant positive correlations were also obtained, between EDa and the lignin content (r = 0.811; *P*<0.05; *n* =8) while this parameter did not appear to significantly relate to xylan, nonetheless a negative trend could be observed. Interestingly, the statistical analysis indicates that glucose conversion was significantly and negatively correlated with xylan (r = -0.726; *P*<0.05; *n* =8) in downward direction from pretreated to the untreated samples as the main physicochemical response of the PSR pretreatment (Figure 4). In a similar way, strong correlation was found between the MW and glucose yield (r = 0.936; *P*<0.01; *n*=8) indicating consistency of the trend observed. Among other structural characteristics, a positive effect on glucose conversion could be observed, even if not significant, ranking in terms of their Pearson's coefficient as S/G ratio < % CrI < EDa, following the same

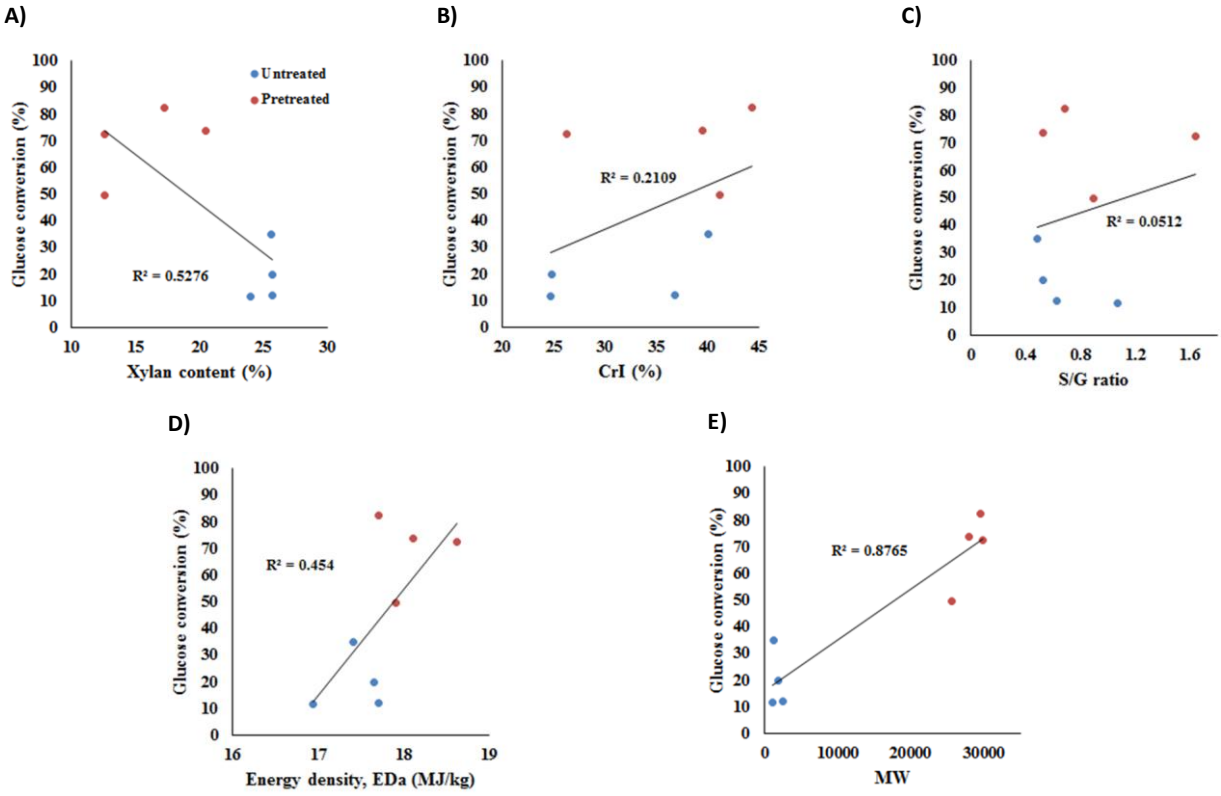

Figure 4. Correlation between % glucose conversion on % xylan content (A), crystallinity index (CrI) (B), S/G ratio (C), "ash-free" energy density (EDa) (D) and molecular weight (E) from untreated and pretreated biomass. Untreated = blue points; Pretreated = red points.

trend with R^2.

Therefore, it can be deduced that the positive effect of the lignin content can be attributed to the reduced hemicellulose-cellulose cross-linking after pretreatment, promoting an increase in the xylan and lignin interactions. Furthermore, high digestibility could be associated with lignin movement and relocalization, increasing cell wall porosity, augmented surface area and improved accessibility of cellulose to enzymes. Higher lignin content due to an hemicellulose removal after an autohydrolysis and/or steam explosion pretreatment seems more important than lignin removal as in other processes (e.g. alkaline pretreatments) for creating cellulases-accessible pores [19,28]. Together, these results demonstrated that xylan content negatively affects the hydrolysis process, whereas efficient enzymatic saccharification was observed in spite of only a partial removal/dissolution of lignin and high MW. Biomass composition therefore plays an important role in the process, but the contributions and interactions of other factors (S/G ratio, % CrI and EDa) should not be neglected. Finally, after PSR-pretreatment, xylan was removed while the lignin was rearranged in the plant cell and after SSF, the final residue can be considered as mainly lignin composed of aromatic compounds (as shown in ESI Table S1) that can be used to generate value-added products and benefit the global economy of the biorefinery.

Bisabolene production from PSR pretreated biomass at high solids loading using *Rhodosporidium toruloides*

Ethanol production from LCB-pretreated hydrolysates after enzymatic hydrolysis has been widely studied using different microorganisms (e.g. *Saccharomyces cerevisiae* and *Escherichia coli*).

Numerous strategies have been applied to improve the yields and titers of the process (e.g. simultaneous saccharification and fermentation with a pre-hydrolysis step) and techno-economic analyses for sustainable process development [48]. When compared to ethanol, the data available around production of precursors of advanced biofuels (e.g. bisabolene) from LCB has been much less studied. The production of bisabolene by *R. toruloides* has been reported from a limited number of LCB hydrolysates (corn stover and sorghum) with ionic liquid and alkali pretreatments, under batch [14] and fed-batch [17] modes. Here we evaluated and demonstrated the potential of PSR-pretreated biomass, preferably at high solids loading, to serve as fermentation media for growth of *R. toruloides* and production of bisabolene.

The experiments for bisabolene fermentations started with a 24 h pre-hydrolysis step, using 20% solids loading and the optimized saccharification conditions determined for each PSR-pretreated biomass (Figure 5). The pH of the hydrolysates was then adjusted to 7.5 and supplemented with defined media as source of nitrogen and vitamins before starting the cultivations, leading to a slight dilution of the substrates. The highest monomeric sugars concentrations reached from the studied LCB sources before fermentation were 82.4 g glucose/L and 28.7 g xylose/L, when using WS. The lowest sugar release was observed with SC, resulting in 73.9 g glucose/L and 27.1 g xylose/L after 24 hours of saccharification. During fermentation, simultaneous consumption of glucose and xylose was observed in all LCB, however, xylose was consumed at a much lower rate. There were noticeable differences in the total amounts of sugars consumed after 120 h of fermentation, with an overall higher sugar consumption being observed with SC and CS hydrolysates.

Slightly different maximum cell biomass values were also observed

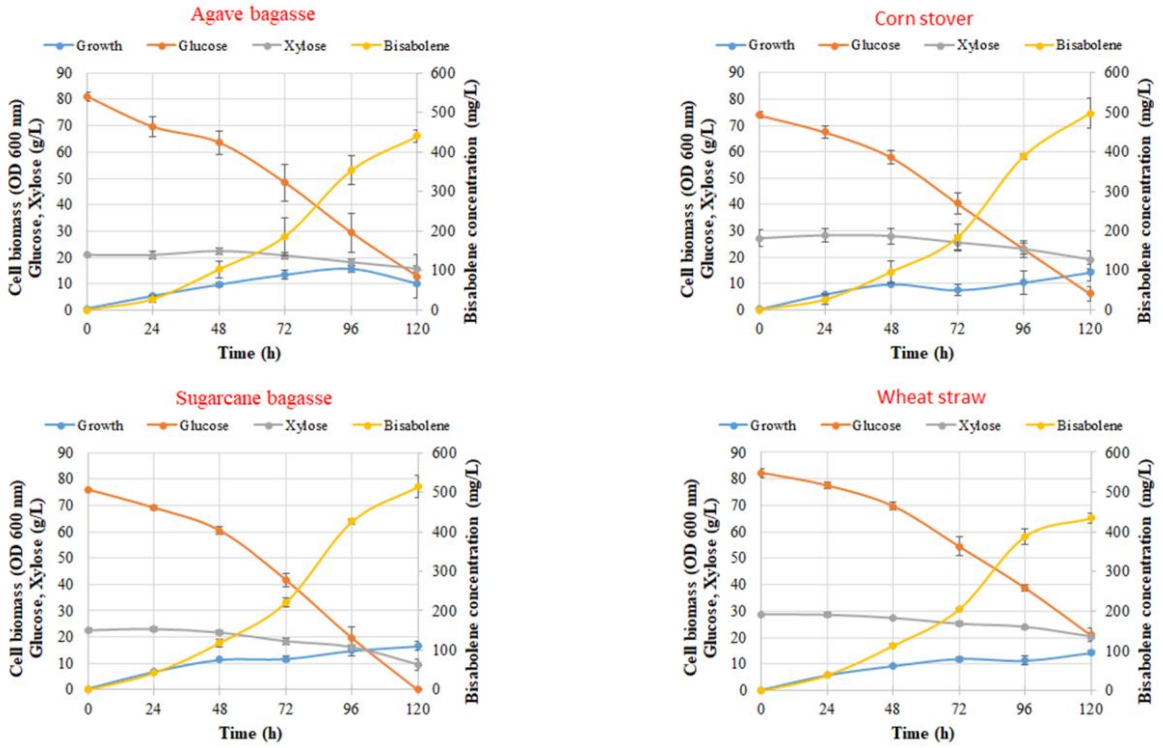

Figure 5. Bisabolene fermentation profiles with *Rhodosporidium toruloides* using hydrolysates from a 20% initial solids loading enzymatic saccharification reaction, with four PSR pretreated biomass sources.

(AG = 15.6, CS = 14.2, SC = 16.7 and WS = 14.2 OD_{600}). Accordingly, the highest production of bisabolene was obtained with SC at 514.1 mg/L, while WS obtained only 434.3 mg/L in the course of 5 days. When compared, the bisabolene production of CS vs. SC and AG vs. WS are statistically different from each other (P <0.05). Statistical differences were also found between CS/SC vs. AG/WS (497-514 and 434-441 mg bisabolene/L, respectively).

The differences in bisabolene production among hydrolysates is attributed to differences in cell growth, microbe nutrient availability and composition and concentration of sugars after saccharification [18]. Hydrolysates from pretreated SC promoted slightly higher growth, sugar consumption and bisabolene production than the other feedstocks. Even if differences in growth and production could be observed, it is important to note that the PSR process coupled to fermentation with *R. toruloides* yielded biocompatible hydrolysates from all tested feedstocks, where the metabolic conversion of sugars into energy, bisabolene and cell biomass were not largely impacted by the type of LCB.

Recently, Yaegashi et al. [(2017)] reported a bisabolene production of ~ 240 mg/L from the hydrolysate of alkali pretreated CS (121 °C, 1 h and 1.5% NaOH) from an initial 17.1 g glucose/L, 9.1 g xylose/L and 383 mg *p*-coumaric acid/L using a 2 L reactor with dissolved oxygen and pH control. The concentration of bisabolene obtained in this study is similar to reports with other organisms (*S. cerevisiae* and *E. coli*) that have undergone extensive modifications through genetic engineering with a production of ~ 400 mg bisabolene/L [49].

The theoretical maximum yield is estimated at 250 mg of bisabolene per gram of glucose, which suggests that there is much room for strain improvement [50]. Furthermore, it has been reported that *R. toruloides* has the ability to grow without inhibition with more than 100 g glucose/L in solution during fermentation, which reveals a high tolerance to osmotic stress [14].

Strain improvement will be one of the most important factors to increase bisabolene titers from *R. toruloides*. This strain is naturally adapted to accumulate high amounts of lipids and other metabolic products, which makes it extremely versatile yet difficult to engineer in ways that allow for higher yields of a single target molecule.

In order to evaluate the growing behaviour of *R. toruloides* at high sugar loading, pretreated WS was selected as the biomass with the higher sugars production during saccharification in the batch experiments LCB into a pulse-feeding strategy to increase solids concentration up to 35%. The profiles of sugar production and bisabolene fermentation from pretreated WS under the pulse-feeding strategy are shown in ESI Figure S4. A 440 mg bisabolene/L was obtained using this strategy from an initial concentration of sugars of 140 g glucose/L and 40 g xylose/L. As shown, this organism is tolerant to high sugar concentrations in hydrolysates, where even small increases in bisabolene and glucose yields obtained by metabolic engineering strategies could have a large impact in the final titers of this compound, making these processes more attractive. Alternative cultivation strategies must therefore be applied to increase the volumetric consumption and production rates and prevent cell lysis, commonly observed after 7 days under these conditions.

Overall, these results indicate that *R. toruloides* is able to grow on and produce bisabolene from all PSR-pretreated biomass hydrolysates and withstand very high initial concentrations of sugars.

Conclusions

This is the first known comparison of PSR conversion efficiency and advanced biofuel production (bisabolene) using four different feedstocks integrated with an in-depth biomass characterization analysis. WS achieved the highest glucose conversion (~82%) while SC obtained the lowest (~51%), which can be strongly correlated (while being statistically significant) to specific structural characteristics such as xylan, lignin and MW when compared to other features (CrI, S/G ratio and EDa) that were reflected on final sugars and bisabolene concentration. These results indicate that this continuous biomass conversion process is promising and may provide a compelling alternative to conventional batch mode unit operations.

Conflicts of interest

There are no conflicts to declare.

Acknowledgements

This work was supported by the Energy Sustainability Fund from the Mexican Secretary of Energy, Grant no. 249564 (Mexican Bioenergy Innovation Center, Bioalcohols Cluster). This work was part of the DOE Joint BioEnergy Institute (http://www.jbei.org) supported by the U.S. Department of Energy, Office of Science, Office of Biological and Environmental Research, through contract DE-AC02-05CH11231 between Lawrence Berkeley National Laboratory and the U.S. Department of Energy. The authors would like to thank the Advanced Biofuels and Bioproducts Process Development Unit (ABPDU) with the energy density analysis.

References

1 A. Karapatsia, I. Pappas, G. Penloglou, O. Kotrotsiou and C. Kiparissides, *Bioenergy Res.*, 2017, **10**, 225–236.
2 L. J. Jönsson and C. Martín, *Bioresour. Technol.*, 2016, **199**, 103–112.
3 S. Sun, S. Sun, X. Cao and R. Sun, *Bioresour. Technol.*, 2016, **199**, 49–58.
4 M. Naresh Kumar, R. Ravikumar, S. Thenmozhi, M. Ranjith Kumar and M. Kirupa Shankar, *Waste and Biomass Valorization*, 2018, 1–17.
5 R. T. Elander, *Aqueous Pretreat. Plant Biomass Biol. Chem. Convers. to Fuels Chem.*, 2013, 417–450.
6 J. Zhang, W. Hou and J. Bao, *Adv. Biochem. Eng. Biotechnol.*, , DOI:10.1007/10.
7 W. Wang, X. Chen, B. S. Donohoe, P. N. Ciesielski, R. Katahira, E. M. Kuhn, K. Kafle, C. M. Lee, S. Park, S. H. Kim, M. P. Tucker, M. E. Himmel and D. K. Johnson, *Biotechnol. Biofuels*, 2014, **7**, 47.
8 S. McIntosh, Z. Zhang, J. Palmer, H. Wong, W. O. S. Doherty and T. Vancov, *Biofuels, Bioprod. Biorefining*, 2016, 346–

358.

9 F. Rodríguez and A. Sánchez, *Modelling of biomass residence time distribution and xylan depolimerization kinetics analysis in a Pilot-Scale Pretreatment Continuous Tubular Reactor*, Elsevier Masson SAS, 2018, vol. 43.

10 F. Carvalheiro, L. C. Duarte, F. Gírio and P. Moniz, in *Biomass Fractionation Technologies for a Lignocellulosic Feedstock Based Biorefinery*, ed. S. I. Mussatto, Elsevier, Amsterdam, 2016, pp. 315–347.

11 T. Pielhop, J. Amgarten, P. R. Von Rohr and M. H. Studer, *Biotechnol. Biofuels*, 2016, **9**, 1–13.

12 R. Agrawal, A. Satlewal, R. Gaur, A. Mathur, R. Kumar, R. P. Gupta and D. K. Tuli, *Biochem. Eng. J.*, 2015, **102**, 54–61.

13 M. H. Thomsen, A. Thygesen, H. Jørgensen, J. Larsen, B. H. Christensen and A. B. Thomsen, *Appl. Biochem. Biotechnol.*, 2006, **129**–**132**, 448–460.

14 E. Sundstrom, J. Yaegashi, J. Yan, F. Masson, G. Papa, A. Rodriguez, M. Mirsiaghi, L. Liang, Q. He, D. Tanjore, T. R. Pray, S. Singh, B. Simmons, N. Sun, J. Magnuson and J. Gladden, *Green Chem.*, , DOI:10.1039/c8gc00518d.

15 A. Sluiter, B. Hames, R. Ruiz and C. Scarlata, *Lab. Anal. Proced. Natl. Renew. Energy Lab. Golden, CO, NREL/ TP-510-42618.*

16 J. A. Perez-Pimienta, C. A. Flores-Gómez, H. A. Ruiz, N. Sathitsuksanoh, V. Balan, L. da Costa Sousa, B. E. Dale, S. Singh and B. A. Simmons, *Bioresour. Technol.*, 2016, **211**, 216–223.

17 J. Yaegashi, J. Kirby, M. Ito, J. Sun, T. Dutta, M. Mirsiaghi, E. R. Sundstrom, A. Rodriguez, E. Baidoo, D. Tanjore, T. Pray, K. Sale, S. Singh, J. D. Keasling, B. A. Simmons, S. W. Singer, J. K. Magnuson, A. P. Arkin, J. M. Skerker and J. M. Gladden, *Biotechnol. Biofuels*, 2017, 1–13.

18 H. Zabed, J. N. Sahu, A. N. Boyce and G. Faruq, *Renew. Sustain. Energy Rev.*, 2016, **66**, 751–774.

19 F. Adani, G. Papa, A. Schievano, G. Cardinale, G. D. D'Imporzano and F. Tambone, *Environ. Sci. Technol.*, 2011, **45**, 1107–1113.

20 L. J. Jönsson, B. Alriksson and N.-O. Nilvebrant, *Biotechnol. Biofuels*, 2013, **6**, 16.

21 G. Cheng, P. Varanasi, C. Li, H. Liu, Y. B. Melnichenko, B. A. Simmons, M. S. Kent and S. Singh, *Biomacromolecules*, 2011, **12**, 933–941.

22 J. A. Perez-Pimienta, M. G. Lopez-Ortega, J. A. Chavez-Carvayar, P. Varanasi, V. Stavila, G. Cheng, S. Singh and B. A. Simmons, *Biomass and Bioenergy*, 2015, **75**, 180–188.

23 Y. Pu, F. Hu, F. Huang, B. H. Davison and A. J. Ragauskas, *Biotechnol. Biofuels*, 2013, **6**, 15.

24 N. Xu, W. Zhang, S. Ren, F. Liu, C. Zhao, H. Liao, Z. Xu, J. Huang, Q. Li, Y. Tu, B. Yu and Y. Wang, *Biotechnol. Biofuels*, 2012, 1–12.

25 Y. Yu and H. Wu, *Ind. Eng. Chem. Res.*, 2010, **49**, 3902–3909.

26 J. S. Lupoi, S. Singh, R. Parthasarathi, B. A. Simmons and R. J. Henry, *Renew. Sustain. Energy Rev.*, 2015, **49**, 871–906.

27 J. S. Lupoi and E. A. Smith, *Appl. Spectrosc.*, 2012, **66**, 903–910.

28 G. Papa, P. Varanasi, L. Sun, G. Cheng, V. Stavila, B. Holmes, B. A. Simmons, F. Adani and S. Singh, *Bioresour. Technol.*, 2012, **117**, 352–359.

29 J. C. del Río, J. Rencoret, P. Prinsen, Á. T. Martínez, J. Ralph and A. Gutiérrez, *J. Agric. Food Chem.*, 2012, **60**, 5922–5935.

30 J. A. Pérez-pimienta, R. M. Mojica-álvarez, L. M. Sánchez-herrera and A. Mittal, *BioEnergy Res.*

31 R. J. Sammons, D. P. Harper, N. Labbé, J. J. Bozell, T. Elder and R. T. G., *BioResources*, 2013, **8**, 2752–2767.

32 M. Li, Y. Pu and A. J. Ragauskas, *Front. Chem.*, 2016, **4**, 1–8.

33 J. Rencoret, G. Marques, A. Gutiérrez, L. Nieto, J. I. Santos, J. Jiménez-Barbero, Á. T. Martínez and J. C. del Río, *Holzforschung*, 2009, **63**, 691–698.

34 J. C. del Río, A. Gutiérrez, I. M. Rodríguez, D. Ibarra and Á. T. Martínez, *J. Anal. Appl. Pyrolysis*, 2007, **79**, 39–46.

35 X. Eduardo, K. Youngmi and L. M. R., in *Aqueous Pretreatment of Plant Biomass for Biological and Chemical Conversion to Fuels and Chemicals*, Wiley-Blackwell, 2013, pp. 39–60.

36 J. L. Gardner, W. He, C. Li, J. Wong, K. L. Sale, B. A. Simmons, S. Singh and D. Tanjore, *RSC Adv.*, 2015, **5**, 51092–51101.

37 A. Anukam, S. Mamphweli, P. Reddy, E. Meyer and O. Okoh, *Renew. Sustain. Energy Rev.*, 2016, **66**, 775–801.

38 P. Mckendry, 2002, **83**, 37–46.

39 L. Axelsson, M. Franzén, M. Ostwald, G. Berndes, G. Lakshmi and N. H. Ravindranath, *Biofuels, Bioprod. Biorefining*, 2012, **6**, 246–256.

40 P. Sannigrahi and A. J. Ragauskas, *Aqueous Pretreat. Plant Biomass Biol. Chem. Convers. to Fuels Chem.*, 2013, 201–222.

41 B. Qi, X. Chen, F. Shen, Y. Su and Y. Wan, *Ind. Eng. Chem. Res*, 2009, **48**, 7346–7353.

42 B. Karki, D. Maurer, T. H. Kim and S. Jung, *Bioresour. Technol.*, 2011, **102**, 1228–1233.

43 K. Pandiyan, R. Tiwari, S. Singh, P. K. S. Nain, S. Rana, A. Arora, S. B. Singh and L. Nain, *Enzyme Res.*

44 M. Marcos, M. T. García-Cubero, G. González-Benito, M. Coca, S. Bolado and S. Lucas, *J Chem Technol Biotechnol*, , DOI:10.1002/jctb.3820.

45 S. Hou and L. Li, *J. Integr. Plant Biol.*, 2011, **53**, 166–175.

46 Q. Yu, X. Tan, X. Zhuang, Q. Wang, W. Wang, W. Qi, G. Zhou, Y. Luo and Z. Yuan, *Bioresour. Technol.*, 2016, **221**, 111–120.

47 F. Araya, E. Troncoso, R. Teixeira and J. Freer, *Biotechnol. Bioeng.*, 2015, **112**, 1783–1791.

48 M. Rastogi and S. Shrivastava, *Renew. Sustain. Energy Rev.*, 2017, **80**, 330–340.

49 P. P. Peralta-Yahya, M. Ouellet, R. Chan, A. Mukhopadhyay, J. D. Keasling and T. S. Lee, *Nat. Commun.*, 2011, **2**, 483–488.

50 B. Özaydin, H. Burd, T. S. Lee and J. D. Keasling, *Metab. Eng.*, 2013, **15**, 174–183.

TABLE OF CONTENTS

Bisabolene bioconversion is demonstrated using pilot-scale hydrothermal pretreated biomass using four feedstocks with in-depth characterization analysis.